Research

Authors for correspondence:
Tung T. Nguyen
e-mail: tungtn@hcmut.edu.vn
Nam T. S. Phan
e-mail: ptsnam@hcmut.edu.vn

Alternative pathways to α,β-unsaturated ketones via direct oxidative coupling transformation using Sr-doped LaCoO₃ perovskite catalyst

Khang H. Trinh, Son H. Doan, Tien V. Huynh,
Phuong H. Tran, Diep N. Pham, Minh-Vien Le,
Tung T. Nguyen and Nam T. S. Phan

Faculty of Chemical Engineering, HCMC University of Technology, VNU-HCM,
268 Ly Thuong Kiet, District 10, Ho Chi Minh City, Viet Nam

M-VL, 0000-0002-6651-0121; TTN, 0000-0002-0912-9981;
NTSP, 0000-0002-5928-7638

A strontium-doped lanthanum cobaltite perovskite material was prepared, and used as a recyclable and effective heterogeneous catalyst for the direct oxidative coupling of alkenes with aromatic aldehydes to produce α,β-unsaturated ketones. The reaction afforded high yields in the presence of di-*tert*-butylperoxide as oxidant. Single oxides or salts of strontium, lanthanum and cobalt, and the undoped perovskite offered a lower catalytic activity than the strontium-doped perovskite. Benzaldehyde could be replaced by benzyl alcohol, dibenzyl ether, 2-oxo-2-phenylacetaldehyde, 2-bromoacetophenone or (dimethoxymethyl) benzene in the oxidative coupling reaction with alkenes. To our best knowledge, reactions between these starting materials with alkenes are new and unknown in the literature.

1. Introduction

α,β-Unsaturated ketones and their derivatives are precious structures, predominantly distributed in numerous biologically active natural products, medicinal chemicals, agricultural chemicals and functional organic materials [1–3]. These structures also serve as starting materials for the synthesis of many valuable organic chemicals [4–6]. Classically, they were synthesized via condensation reactions in the presence of stoichiometric amounts

of strong bases, thus suffering several severe drawbacks [7]. Accordingly, considerable efforts have been devoted to achieve more efficient and greener synthetic pathways to these significant compounds. Some recent protocols include platinum-catalysed tandem hydroformylation/aldol condensation reaction of vinyl aromatics and ketones [8], Doebner–Knoevenagel type condensation reactions in the presence of acyl/aroyl Meldrum's acid [9], copper-catalysed Saegusa-type oxidation of enol acetates [10], zeolite-catalysed tandem hydration/condensation of alkynes and aldehydes [11] and IBX-catalysed dehydration of allylic hydroperoxides [12]. Among numerous synthetic approaches, reactions via direct C–H bond activation have been explored, as the prefunctionalization of reactants and the purification of intermediates could be minimized [13–15]. Previously, Wang *et al.* developed the homogeneous copper-catalysed direct oxidative coupling of alkenes with aldehydes to produce α,β-unsaturated ketones (scheme 1a) [16]. In this protocol, neither the aldehydes nor the alkenes need to be prefunctionalized, therefore offering advantages over conventional synthetic strategies.

Perovskites have emerged as a significant family of materials with fascinating physico-chemical properties, such as electron mobility, redox performance, thermal stability, and electronic and ionic conductivity [17–19]. They are complex metal oxides with the general formula of ABO_3, where A normally stands for an alkaline-earth or rare-earth metal cation, and B represents a transition metal [20,21]. In these structures, partial or full substitution of the A or B cation leads to different interesting properties [22]. In the catalysis field, perovskites have been extensively studied for reduction–oxidation transformations for many years, including CO oxidation [23–26], reforming of methane [27–30], production of hydrogen [31–33], removal of volatile organic compounds [34–36], wastewater treatment [37–40] water splitting [41–44] and oxygen reduction reaction [45–48]. Nevertheless, the utilization of perovskites as catalysts for organic synthesis is *extremely rare* in the literature. In this study, we would like to report the application of a strontium-doped lanthanum cobaltite perovskite as a recyclable heterogeneous catalyst for the direct oxidative coupling of alkenes with aromatic aldehydes to produce α,β-unsaturated ketones (scheme 1b). It should be noted that single oxides or salts of strontium, lanthanum and cobalt, and the undoped perovskite exhibited lower activity than the strontium-doped perovskite. Interestingly, we found that aromatic aldehydes could be replaced by several starting materials in the perovskite-catalysed direct oxidative coupling reaction (scheme 1c–g). To our best knowledge, reactions between these starting materials and alkenes are new and unknown in the literature.
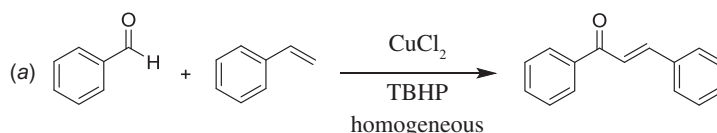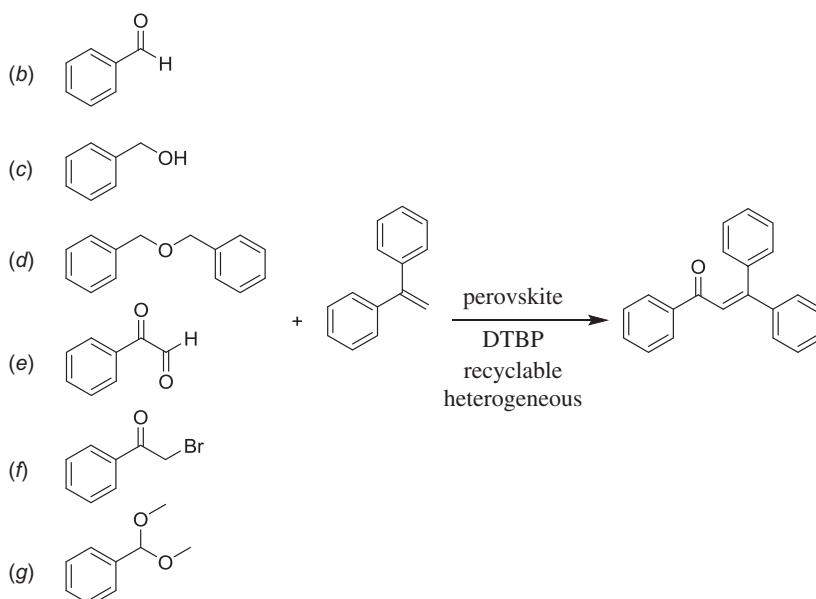
Previous work [16]:

This work:

Scheme 1. The difference between previous work and this work.

2. Experimental set-up

2.1. Synthesis of strontium-doped lanthanum cobaltite perovskite catalyst

The strontium-doped lanthanum cobaltite perovskite powder was prepared via gelation and calcination approach [49]. The nitrate salts of lanthanum (La(NO$_3$)$_3$.6H$_2$O, 3.90 g, 0.009 mol), strontium (Sr(NO$_3$)$_2$, 1.28 g, 0.006 mol) and cobalt (Co(NO$_3$)$_2$.6H$_2$O, 4.45 g, 0.015 mol) were dissolved in deionized water (100 ml) with vigorous stirring. Subsequently, citric acid (11.3 g, 0.06 mol) as a chelating agent was added to the solution. The resulting mixture was then heated at 80°C under continuous stirring for 4 h in a water bath, and the clear pink solution was transformed into a red gel. After the gelation step, the red gel was burnt at 140°C overnight in an electric oven to produce soft-ash form. In order to obtain the perovskite, the ash was pre-calcined at 400°C for 0.5 h, pulverized, and then calcined at 500°C under air for 8 h. The resulting powder was consequently ball-milled in ethanol media using 5 mm diameter zirconia balls for 12 h at room temperature, and dried overnight in an electric oven at 140°C to achieve the strontium-doped lanthanum cobaltite perovskite (La$_{0.6}$Sr$_{0.4}$CoO$_3$, 2.56 g).

2.2. Catalytic studies

In a representative experiment, a mixture of 1,1-diphenylethylene (0.0541 g, 0.3 mmol) and diphenyl ether (16 μl, 0.1 mmol) as an internal standard in benzaldehyde (1 ml) was added into a pressurized vial. The reaction mixture was magnetically stirred and heated for 5 min. The strontium-doped lanthanum cobaltite perovskite catalyst (3.4 mg, 5 mol%) was then added into the vial. The reaction mixture was magnetically stirred for 2 min to disperse entirely the catalyst in the liquid phase, followed by the addition of di-*tert*-butylperoxide (DTBP; 0.27 ml, 1.2 mmol). The resulting mixture was continuously stirred at 120°C for 18 h under air. Upon completion of the reaction step, the reaction mixture was diluted with ethyl acetate (5 ml) and washed with saturated NaHCO$_3$ solution (5 ml). The ethyl acetate layer was dried by anhydrous Na$_2$SO$_4$. Reaction yields were recorded from GC analysis results regarding the diphenyl ether internal standard. To isolate the coupling product, the ethyl acetate solution was concentrated under vacuum and purified by column chromatography on silica gel with hexane/ethyl acetate solvent mixture. The structure of the coupling product was analysed by GC-MS, ^{1}H NMR and ^{13}C NMR. The La$_{0.6}$Sr$_{0.4}$CoO$_3$ catalyst was separated from the reaction mixture by centrifugation, washed carefully with ethylacetate, acetone and diethyl ether, dried under vacuum at room temperature overnight on a Schlenkline, and re-used to investigate the possibility of catalyst recycling.

3. Results and discussion

3.1. Catalyst synthesis and characterization

The strontium-doped lanthanum cobaltite perovskite powder was characterized using conventional analysis methods. Scanning electron microscopy (SEM) studies indicated that particles are of inhomogeneous size, highly agglomerated, forming irregular lumps (figure 1). Energy-dispersive X-ray (EDX) investigation confirmed the presence of La, Sr, Co and O elements in the structure of the perovskite with La : Sr : Co molar ratio of 0.63 : 0.37 : 1.07 being recorded (figure 2). Additionally, ICP analysis of the bulk sample indicated a La : Sr : Co molar ratio of 0.63 : 0.38 : 1.0. These data are in good agreement with the designed ratio of 0.60 : 0.40 : 1.0, confirming the La$_{0.6}$Sr$_{0.4}$CoO$_3$ formula for the material. Nitrogen physisorption measurements of the La$_{0.6}$Sr$_{0.4}$CoO$_3$ sample revealed Langmuir surface areas of less than 10 m^2 g^{-1} (figure 3). X-ray diffraction (XRD) patterns (figure 4) showed the presence of the typical LaCoO$_3$ perovskite diffraction peaks at 2θ of 23.3°, 32.9°, 40.7°, 47.4° and 48.8°. However, the XRD patterns also suggested that the material contained impurities phases of SrO (at 2θ of 29.5° and 35.2°) and La$_2$O$_3$ (at 2θ of 50.0°). The analysis results verified that La$_{0.6}$Sr$_{0.4}$CoO$_3$ is well indexed to perovskite structure of LaCoO$_3$ (JCPDS 82–1961). Certainly, XRD result of the La$_{0.6}$Sr$_{0.4}$CoO$_3$ is consistent with the literature [49–51]. Fourier-transform infrared spectroscopy (FT-IR) spectra of the La$_{0.6}$Sr$_{0.4}$CoO$_3$ in the region between 4000 and 500 cm^{-1} are identical to those previously reported in the literature (figure 5) [52]. The absorption bands at 574 cm^{-1} correspond to the deformation modes of LaCoO$_3$. Another absorption peak at 420 cm^{-1} (not shown here) marks the formation of O–Co–O and La–O–Co, indicating that LaCoO$_3$ structure was generated [53]. The strong absorption peak at 1454 cm^{-1} is due to the vibrations of the lanthanum cobaltite crystal lattice [54].
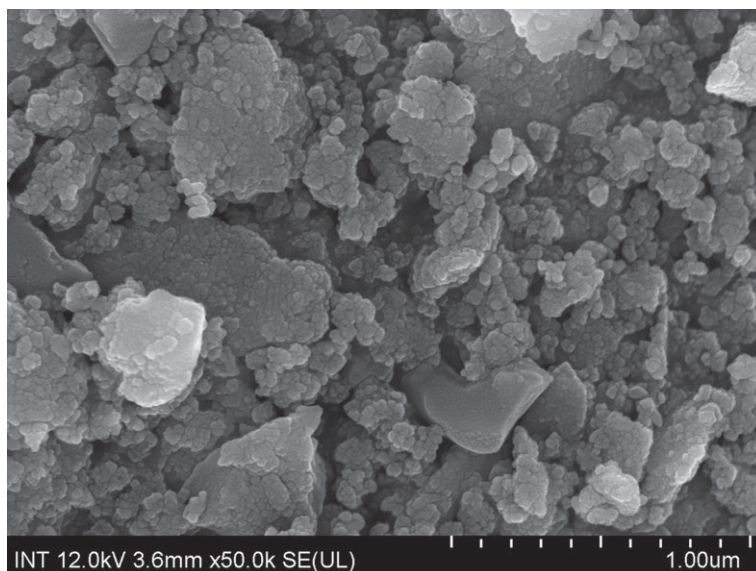
Figure 1. SEM micrograpth of the $La_{0.6}Sr_{0.4}CoO_3$ perovskite catalyst.

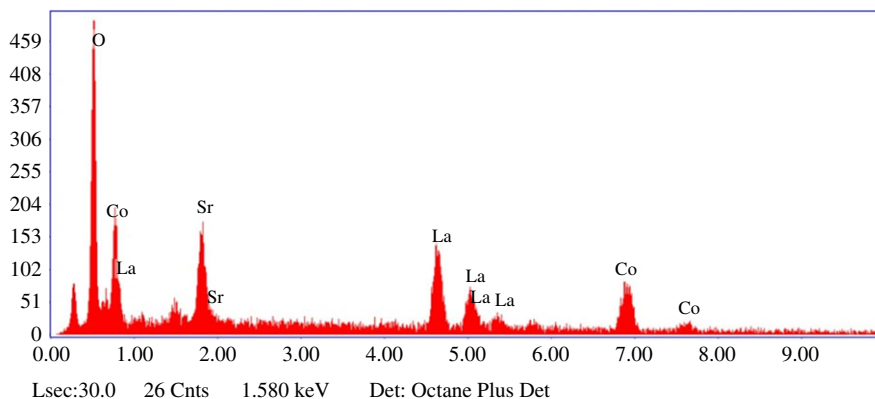**Figure 2.** EDX patterns of the $La_{0.6}Sr_{0.4}CoO_3$ perovskite catalyst.

A band at 667 cm^{-1} was observed on the sample, assigned to Co_3O_4, which was generated due to strontium doping in the perovskite [55]. Thermal gravimetric analysis (TGA) result verified that the material was thermally stable up to 600°C (figure 6). Transmission electron microscopy (TEM) studies showed a regular shape of the material with the nanosize of 5–15 nm (figure 7).

3.2. Catalytic studies

The strontium-doped lanthanum cobaltite perovskite was used as a heterogeneous catalyst for the direct oxidative coupling of benzaldehyde with 1,1-diphenylethylene to produce 1,3,3-triphenylprop-2-en-1-one as the major product (scheme 1b). The transformation required the presence of an oxidant, and a quick test indicated that DTBP was appropriate for the reaction system. Initially, reaction conditions were screened to maximize the yield of the coupling product (electronic supplementary material, table S1). The impact of temperature on the formation of the α,β-unsaturated ketone was studied by performing the reaction at different temperatures, ranging from ambient temperature to 140°C (figure 8). The reaction was carried out under air for 18 h, in the presence of 5 mol% perovskite-based catalyst, with four equivalents of DTBP as oxidant. In this protocol, excess benzaldehyde served as both reactant and solvent for the reaction, and no additional organic solvent was required. It was noted that no trace amount of the coupling product was detected for the reaction conducted at room temperature. Boosting the temperature significantly accelerated the coupling reaction, and best yield of 1,3,3-triphenylprop-2-en-1-one was obtained for the reaction performed at 120°C. Nevertheless, considerably lower yield was recorded when the reaction temperature was increased to 140°C. Indeed, GC-MS analysis of the reaction
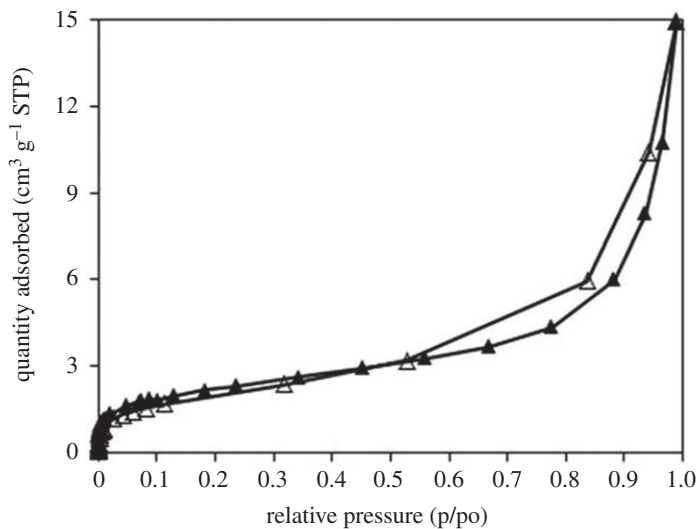
Figure 3. Nitrogen adsorption/desorption isotherm of the $La_{0.6}Sr_{0.4}CoO_3$ perovskite. Adsorption data are shown as closed triangles and desorption data as open triangles.
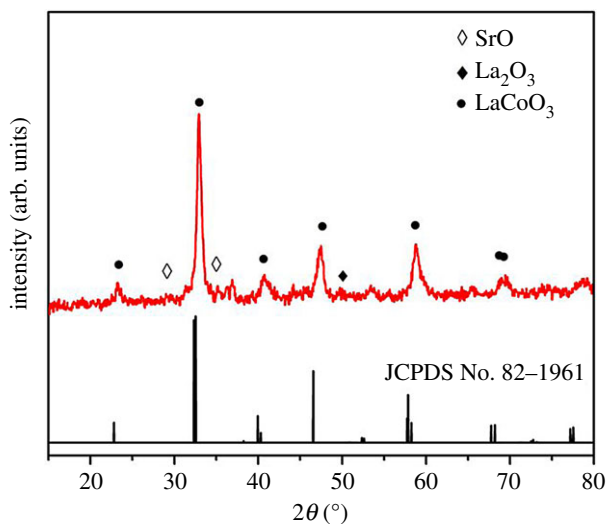

Figure 4. XRD patterns of the $La_{0.6}Sr_{0.4}CoO_3$ perovskite catalyst.

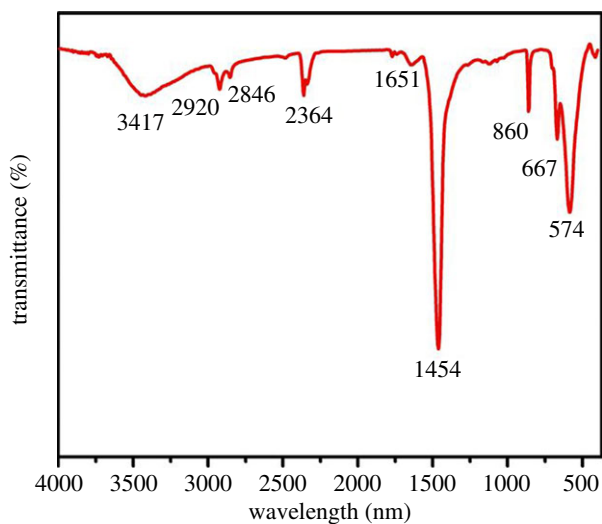**Figure 5.** FT-IR spectra of the $La_{0.6}Sr_{0.4}CoO_3$ perovskite catalyst.

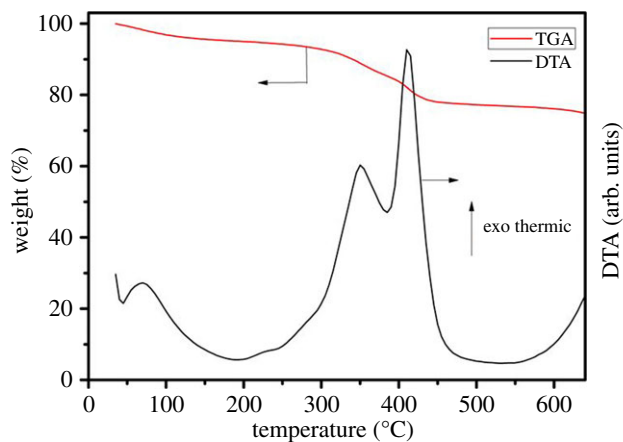**Figure 6.** TGA of the $La_{0.6}Sr_{0.4}CoO_3$ perovskite catalyst.
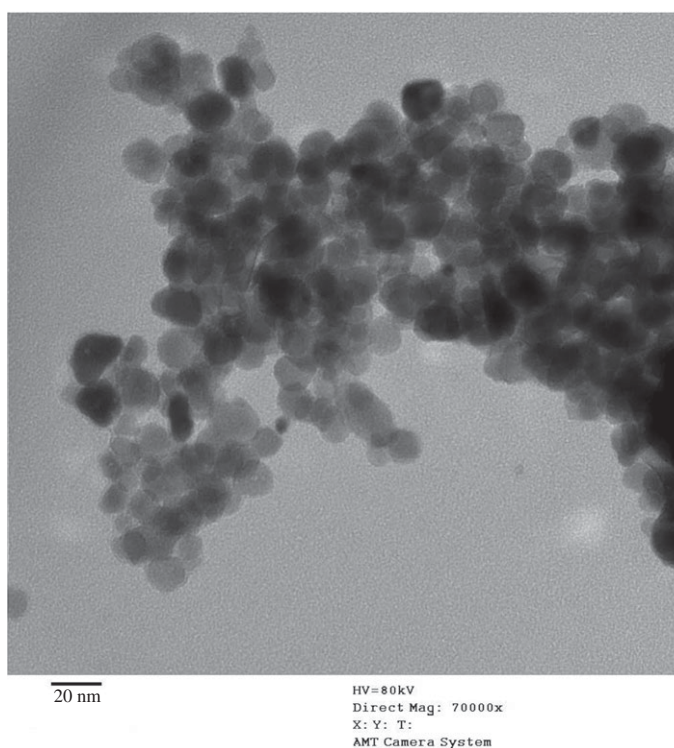

HV=80kV
Direct Mag: 70000x
X: Y: T:
AMT Camera System

Figure 7. TEM micrograph of the $La_{0.6}Sr_{0.4}CoO_3$ perovskite catalyst.

mixture indicated the presence a large amount of benzophenone, implying that the oxidation of 1,1-diphenylethylene was significant under this condition.

It was noted that the coupling reaction could not progress in the absence of the oxidant, with only 7% yield of 1,3,3-triphenylprop-2-en-1-one being detected. A series of oxidants were tested for the reaction in order to maximize the yield of the α,β-unsaturated ketone (figure 9). The reaction using $K_2S_2O_8$ as oxidant afforded 60% yield, while $AgNO_3$, H_2O_2 and oxygen were not suitable for this transformation. Indeed, in the previous homogeneous copper-catalysed direct oxidative coupling of alkenes with aldehydes to produce α,β-unsaturated ketones, Wang *et al*. employed *tert*-butyl hydroperoxide as the oxidant [16]. However, in this work, it was observed that the reaction using the strontium-doped lanthanum cobaltite perovskite proceeded slowly in the presence of this oxidant, with 20% and 10% yields being recorded for the case of *tert*-butyl hydroperoxide in water and *tert*-butyl hydroperoxide in decane, respectively. *tert*-Butyl peroxybenzoate and cumyl hydroperoxide also displayed low performance as the oxidant. In this oxidant series, DTBP emerged as the best option, producing the desired α,β-unsaturated ketone in 80% yield. Next, the influence of oxidant amount on the reaction was studied (figure 10). It should be
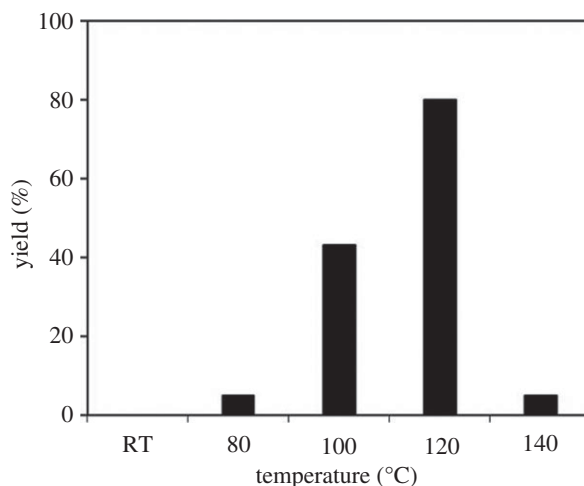
Figure 8. Yields of 1,3,3-triphenylprop-2-en-1-one at different temperatures. Reaction conditions: 1,1-diphenylethylene (0.3 mmol); benzaldehyde (1 ml); DTBP (1.2 mmol); catalyst (5 mol%); 18 h; under air. Best yield was achieved at 120°C.
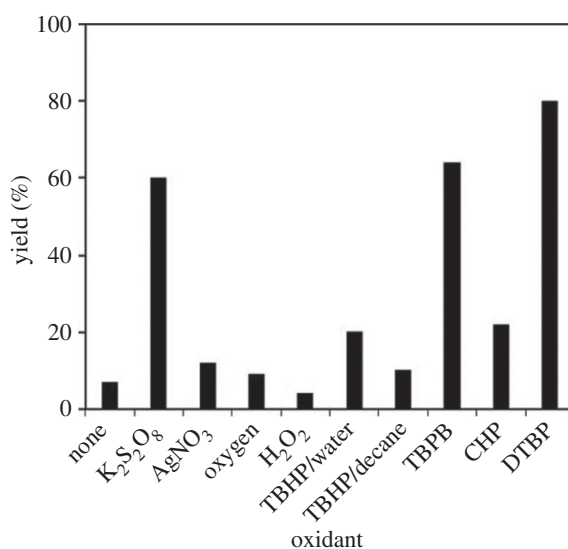

Figure 9. Yields of 1,3,3-triphenylprop-2-en-1-one with different oxidants. Reaction conditions: 1,1-diphenylethylene (0.3 mmol); benzaldehyde (1 ml); oxidant (1.2 mmol); catalyst (5 mol%); 120°C; 18 h; under air. Best yield was achieved with DTBP.

noted that only 5% yield was detected in the absence of the oxidant. Expanding the amount of the oxidant led to higher yields, and best yield was achieved with four equivalents of DTBP.

From these results, the amount of the strontium-doped lanthanum cobaltite perovskite catalyst was consequently adjusted to improve the yield of the desired α,β-unsaturated ketone product (figure 11). In the previous homogeneous copper-catalysed direct oxidative coupling of alkenes with aldehydes to produce α,β-unsaturated ketones, Wang *et al.* used up to 20 mol% $CuCl_2$ catalyst for the reaction [16]. Without the catalyst, no trace quantity of product was recorded, verifying the indispensability of the perovskite-based material for the reaction. Using 1 mol% catalyst, 17% yield was detected, and this value was improved to 55% with 3 mol% catalyst. The yield was enhanced to 80% when increasing the catalyst amount to 5 mol%. Nevertheless, extending the catalyst amount to more than 5 mol% did not lead to a higher yield of 1,3,3-triphenylprop-2-en-1-one. Additionally, in this procedure, excess benzaldehyde was used as both reactant and solvent for the reaction. We also explored the coupling reaction in different solvents. For reactions using solid catalysts, the polarity, as well as the structure of solvents, might considerably control the yield and selectivity of the reaction [56]. A series of solvents were tested for the reaction using the strontium-doped lanthanum cobaltite perovskite catalyst under standard conditions (figure 12). Interestingly, it was found that using an additional solvent significantly decelerated the transformation, and the best result was achieved with neat conditions.
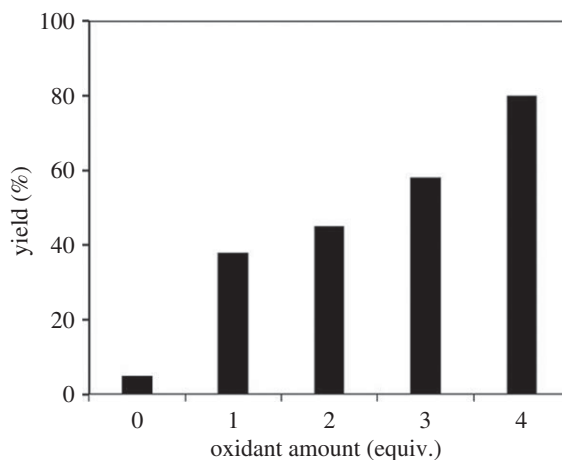
Figure 10. Yields of 1,3,3-triphenylprop-2-en-1-one at different oxidant amounts. Reaction conditions: 1,1-diphenylethylene (0.3 mmol); benzaldehyde (1 ml); catalyst (5 mol%); 120°C; 18 h; under air. Best yield was achieved with four equivalents of DTBP.
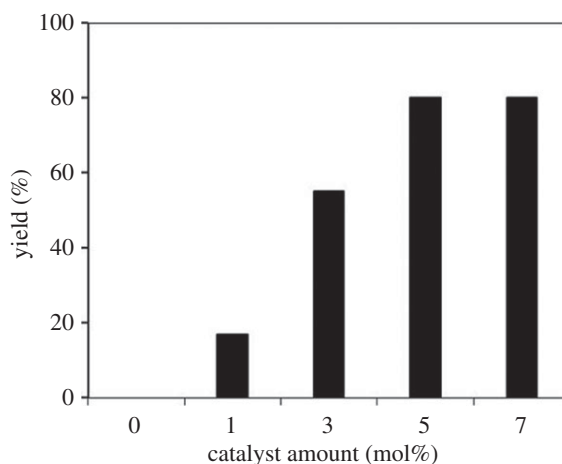

Figure 11. Yields of 1,3,3-triphenylprop-2-en-1-one at different catalyst amounts. Reaction conditions: 1,1-DiphenylEthylene (0.3 mmol); benzaldehyde (1 ml); DTBP (1.2 mmol); 120°C; 18 h; under air. Best yield was achieved with 5 mol% catalyst.

Since the direct oxidative coupling of benzaldehyde with 1,1-diphenylethylene to produce 1,3,3-triphenylprop-2-en-1-one using the strontium-doped lanthanum cobaltite perovskite catalyst progressed in a liquid phase, a vital point that must be studied is whether the α,β-unsaturated ketone product was generated via truly heterogeneous or to some extent homogeneous conditions. The reaction was carried out at 120°C under air for 18 h, in the presence of 5 mol% perovskite-based catalyst, with four equivalents of DTBP as oxidant. After the first 3 h with 60% yield being recorded, the solid catalyst was isolated by centrifugation, the liquid phase was obtained and transferred to a new and fresh reactor. The mixture was subsequently heated at 120°C under air for 15 h, with samples being collected and analysed by GC. Under these conditions, almost no additional 1,3,3-triphenylprop-2-en-1-one was observed in the reaction mixture (figure 13). These observations confirmed that the direct oxidative coupling of benzaldehyde with 1,1-diphenylethylene using the strontium-doped lanthanum cobaltite perovskite catalyst proceeded via truly heterogeneous conditions, and almost no α,β-unsaturated ketone was produced via homogeneous catalysis.

In order to highlight the superiority of the strontium-doped lanthanum cobaltite perovskite catalyst in the direct oxidative coupling of benzaldehyde with 1,1-diphenylethylene, numerous homogeneous and heterogeneous catalysts were tested (electronic supplementary material, table S2). The reaction was conducted at 120°C under air for 18 h, in the presence of 5 mol% catalyst, with four equivalents of DTBP as oxidant. In iron salt series, using $FeCl_2$ and $FeCl_3$ led to 38% and 43% yields, respectively, while $Fe(NO_3)_3$ and $FeSO_4$ were inactive for the transformation. Similarly, $CuSO_4$, $Cu(NO_3)_2$ and $Ni(NO_3)_2$ exhibited low activity. The three precursors of the strontium-doped lanthanum cobaltite perovskite, $La(NO_3)_2$, $Co(NO_3)_2$ and $Sr(NO_3)_2$, offered low performance, with 1%, 24% and 1% yields being recorded, respective (figure 14). Moving to heterogeneous catalyst series, the reaction using Cu-MOF-74

Figure 12. Yields of 1,3,3-triphenylprop-2-en-1-one in different solvents. Reaction conditions: 1,1-diphenylethylene (0.3 mmol); benzaldehyde (1 ml); DTBP (1.2 mmol); catalyst (5 mol%); 120°C; 18 h; under air. Best yield was achieved under neat conditions.

Figure 13. Leaching test confirmed that no additional product was produced after catalyst removal.

Figure 14. Yields of 1,3,3-triphenylprop-2-en-1-one with different homogeneous catalysts. Reaction conditions: 1,1-diphenylethylene (0.3 mmol); benzaldehyde (1 ml); DTBP (1.2 mmol); catalyst (5 mol%); 120°C; 18 h; under air.
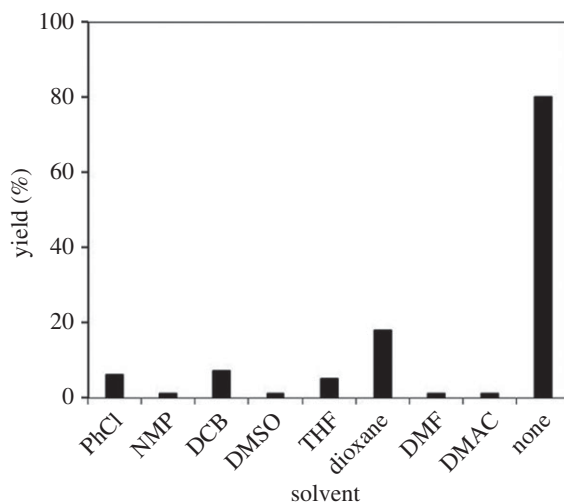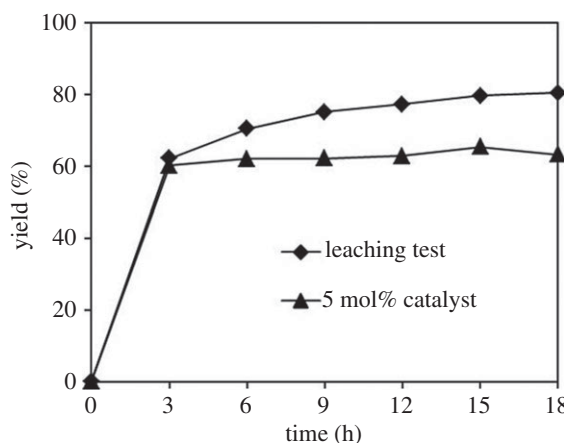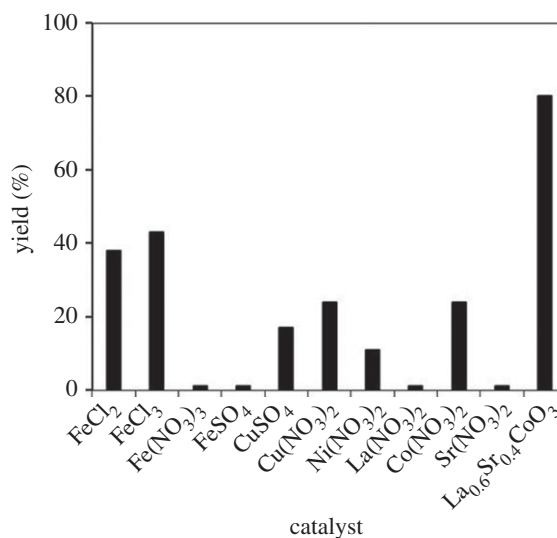
Figure 15. Yields of 1,3,3-triphenylprop-2-en-1-one with different heterogeneous catalysts. Reaction conditions: 1,1-diphenylethylene (0.3 mmol); benzaldehyde (1 ml); DTBP (1.2 mmol); catalyst (5 mol%); 120°C; 18 h; under air.
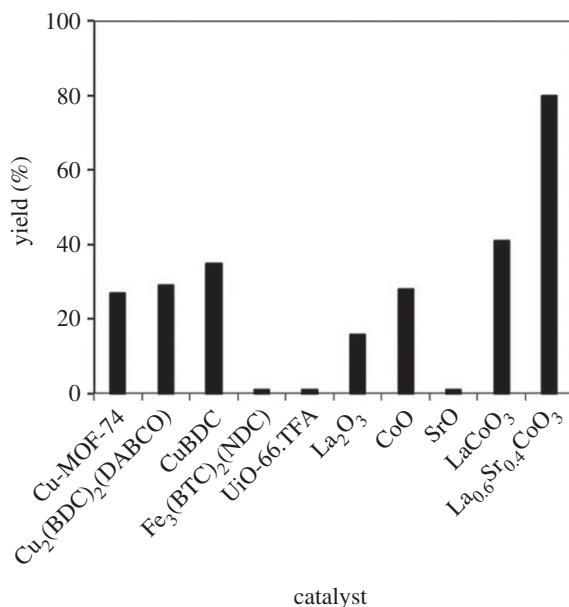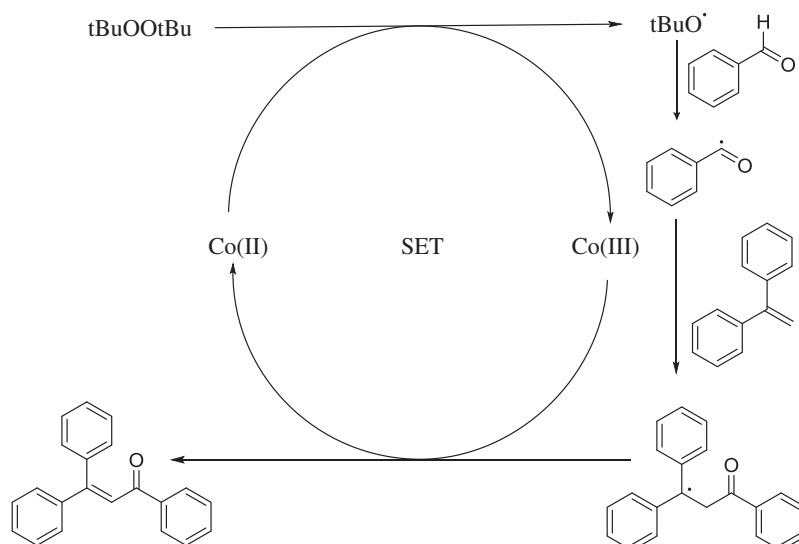

Scheme 2. Proposed reaction pathway.

resulted in 27% yield, while 29% and 35% yields were observed for the case of $Cu_2(BDC)_2(DABCO)$ and Cu(BDC), respectively. Other MOFs, including $(BTC)_2(NDC)$, and UiO-66.TFA were inactive for the reaction. Similarly, the La_2O_3-catalysed reaction produced 1,3,3-triphenylprop-2-en-1-one in 16% yield, while 28% yield was detected for the case of CoO. SrO was noted to be inactive, with only 1% yield being recorded. Using the undoped perovskite, $LaCoCo_3$, led to 41% yield. Compared to other catalysts, the strontium-doped lanthanum cobaltite perovskite was the best option, offering the desired α,β-unsaturated ketone product in 80% yield (figure 15).

Based on previous reports [16,57–59], a plausible mechanism for the $La_{0.6}Sr_{0.4}CoO_3$-catalysed direct oxidative coupling of benzaldehyde with 1,1-diphenylethylene is proposed in scheme 2. Initially, high-temperature decomposition of *tert*-butyl hydroperoxide with the assistance of Co(II) gives a *tert*-butoxy radical, which abstracts a hydrogen atom of benzaldehyde to form a benzoyl radical. Although such an intermediate was proposed in earlier examples, attempts to trap the benzoyl radical have not been successful [16,57]. Notably, using a radical quenching competitor such as TEMPO lowered the yield, thus somewhat confirming the radical mechanism. Addition of the benzoyl radical to ethene-1,1-diyldibenzene generates a new radical, subsequently followed by the direct oxidation of this radical by
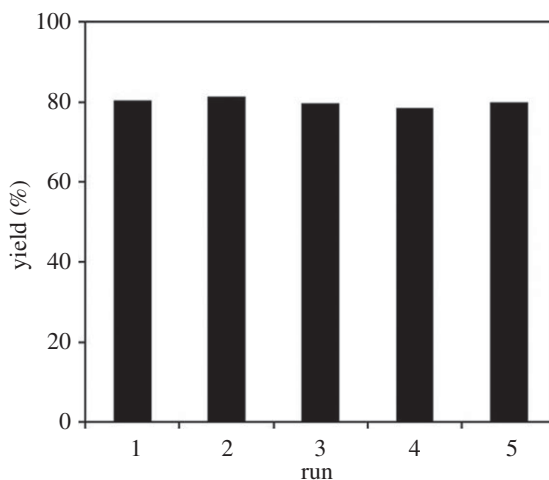
Figure 16. Reutilization of the strontium-doped lanthanum cobaltite perovskite catalyst.
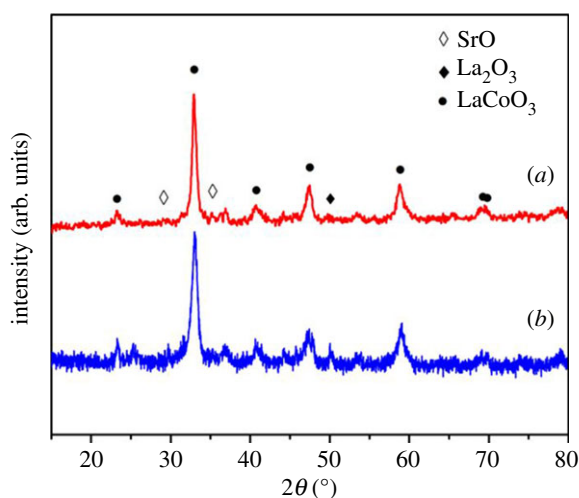
Figure 17. XRD patterns of fresh (*a*) and re-used (*b*) $La_{0.6}Sr_{0.4}CoO_3$ perovskite catalysts.
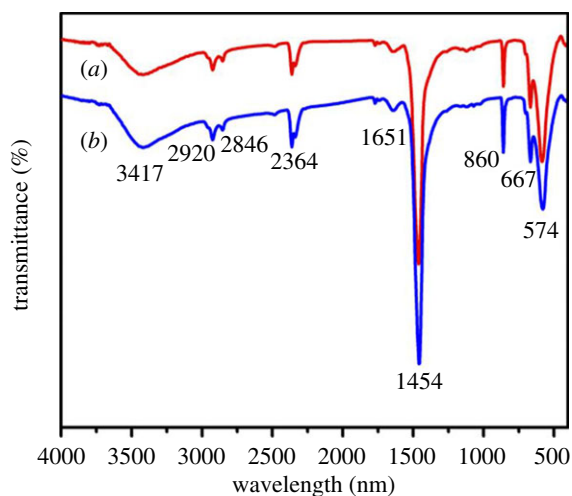
Figure 18. FT-IR spectra of fresh (*a*) and re-used (*b*) $La_{0.6}Sr_{0.4}CoO_3$ perovskite catalysts.

Co(III) and the release of a proton, producing the final coupling product, and regenerating the Co(II) species back to the catalytic cycle. It should be noted the reaction using CoO catalyst afforded 28% yield, while 41% yield was detected for that using $LaCoO_3$ catalyst. Indeed, it was previously reported that B site ion in ABO_3

Table 1. Synthesis of α,β-unsaturated ketones via direct oxidative coupling reactions between 1,1-diphenylethylene and several reactants using the strontium-doped lanthanum cobaltite perovskite catalyst[a]
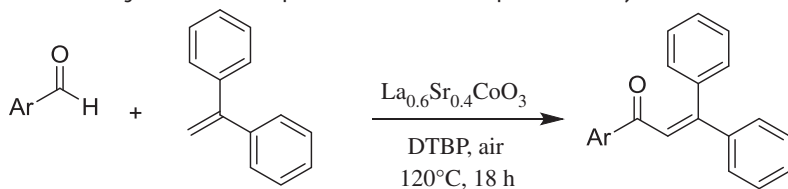
entry	reactant 1	product	yield[b] (%)
1			75
2			76
3			76
4			71
5			73
6			57
7			53

(*Continued.*)

Table 1. (Continued.)

entry	reactant 1	product	yield[b] (%)
8	(dibenzyl ether structure)	(1,3,3-triphenylprop-2-en-1-one structure)	51
9	(phenylglyoxal structure)	(1,3,3-triphenylprop-2-en-1-one structure)	74
10	(benzaldehyde dimethyl acetal structure)	(1,3,3-triphenylprop-2-en-1-one structure)	69
11	(phenacyl bromide structure)	(1,3,3-triphenylprop-2-en-1-one structure)	66

[a]Reaction conditions: reactant (1 ml); 1,1-diphenylethylene (0.3 mmol); DTBP (1.2 mmol); catalyst (5 mol%); 120°C; 18 h; under air.
[b]Isolated yield.

perovskite with high valence would improve the mobility of lattice oxygen, thus enhancing redox activity of catalyst [60]. Moreover, partial substituting La(III) site by Sr(II) site in the LaCoO$_3$ perovskite would additionally increase the mobility of lattice oxygen to attain the charge balance, further facilitating the redox step between Co(III) and Co(II) species in the catalytic cycle [23]. Therefore, the presence of strontium in the lanthanum cobaltite perovskite would considerably increase the catalytic activity in the direct oxidative coupling reaction. As a result, the La$_{0.6}$Sr$_{0.4}$CoO$_3$ exhibited significantly higher catalytic activity than the LaCoO$_3$ as well as the CoO catalyst.

To further underline the strontium-doped lanthanum cobaltite perovskite catalyst in the direct oxidative coupling of benzaldehyde with 1,1-diphenylethylene, a critical issue that must be investigated is the reusability of the catalyst. It was accordingly decided to explore the activity of the catalyst after repeated runs under standard conditions. The reaction was conducted at 120°C under air for 18 h, in the presence of 5 mol% perovskite-based catalyst, with four equivalents of DTBP as oxidant. After the first catalytic experiment, the strontium-doped lanthanum cobaltite perovskite catalyst was separated from the reaction mixture by centrifugation, washed carefully with ethylacetate, acetone, and diethyl ether, dried under vacuum at room temperature overnight on a Schlenkline, and re-used to investigate the possibility of catalyst recycling. It was noted that under standard conditions, the catalyst could be re-used several times for the direct oxidative coupling of benzaldehyde with 1,1-diphenylethylene to produce 1,3,3-triphenylprop-2-en-1-one. Certainly, 80% yield of the desired α,β-unsaturated ketone product was achieved in the fifth catalytic run (figure 16). The recycled catalyst was additionally characterized by XRD, and the result was compared with that of the fresh material. The analysis data verified that the structure of the strontium-doped lanthanum cobaltite perovskite was maintained during the catalytic experiments (figure 17). Additionally, FT-IR spectra of the recycled catalyst were similar to those of the fresh one (figure 18).

With these results, we subsequently expanded the research scope to the direct oxidative coupling reactions between 1,1-diphenylethylene and several reactants using the strontium-doped lanthanum cobaltite perovskite catalyst (table 1). The reaction was conducted at 120°C under air for 18 h, in the

presence of 5 mol% perovskite-based catalyst, with four equivalents of DTBP as oxidant. The α,β-unsaturated ketone product was purified by column chromatography. Using this procedure, 1,3,3-triphenylprop-2-en-1-one was produced in 75% isolated yield (entry 1). Benzaldehydes containing a substituent were also reactive, affording the corresponding product in reasonable yields (entries 2–3). Additionally, heteroaromatic aldehydes such as thiophene-2-carbaldehyde and furan-2-carbaldehyde joined the reaction readily (entries 4–5). Interestingly, we found that several compounds could be used as alternative reactants for this transformation. The reaction of 1,1-diphenylethylene with benzyl alcohol or 4-methylbenzyl alcohol proceeded to 57% and 53% yields, respectively (entries 6–7). Moving to dibenzyl ether, the transformation afforded 1,3,3-triphenylprop-2-en-1-one in 51% yield (entry 8). 2-Oxo-2-phenylacetaldehyde was noted to be less reactive towards the reaction, producing the α,β-unsaturated ketone product in 74% yield (entry 9). Interestingly, (dimethoxymethyl)benzene and 2-bromo-1-phenylethan-1-one were also reactive, with 69% and 66% yields being recorded, respectively (entries 10–11).

4. Conclusion

In this work, a strontium-doped lanthanum cobaltite perovskite material was prepared via gelation and calcination approach, and consequently characterized by several methods. The perovskite was used as a recyclable heterogeneous catalyst for the direct oxidative coupling of alkenes with aromatic aldehydes to produce α,β-unsaturated ketones. High yields were achieved in the presence of DTBP as oxidant. The catalyst was re-used several times without considerable decline in the formation of the α,β-unsaturated ketones. Single oxides or salts of strontium, lanthanum and cobalt, and the undoped perovskite exhibited lower catalytic activity than the strontium-doped perovskite. Interestingly, we found that benzaldehyde could be replaced by benzyl alcohol, dibenzyl ether, benzyl amine, 2-bromoacetophenone or (dimethoxymethyl)benzene in the oxidative coupling reaction with alkenes. Reactions between these alternative starting materials with alkenes were not previously reported. The diversified starting materials of the protocol, in conjunction with a recyclable catalyst, make the synthetic protocol efficient and attractive to the chemical and pharmaceutical industries.

References

1. Zhu M et al. 2018 Design, synthesis, and evaluation of chalcone analogues incorporate α,β-unsaturated ketone functionality as anti-lung cancer agents via evoking ROS to induce pyroptosis. *Eur. J. Med. Chem.* **157**, 1395–1405. (doi:10.1016/j.ejmech.2018.08.072)

2. Yang Z, Fonović M, Verhelst SHL, Blum G, Bogyo M. 2009 Evaluation of α,β-unsaturated ketone-based probes for papain-family cysteine proteases. *Bioorg. Med. Chem.* **17**, 1071–1078. (doi:10.1016/j.bmc.2008.02.089)

3. Choi JW et al. 2015 Synthesis of a series of unsaturated ketone derivatives as selective and reversible monoamine oxidase inhibitors. *Bioorg. Med. Chem.* **23**, 6486–6496. (doi:10.1016/j.bmc.2015.08.012)

4. Han WJ, Pu F, Li CJ, Liu ZW, Fan J, Shi XY. 2018 Carboxyl-directed conjugate addition of C—H bonds to α,β-unsaturated ketones in air and water. *Adv. Synth. Catal.* **360**, 1358–1363. (doi:10.1002/adsc.201701468)

5. Li JY, Kim HY, Oh K. 2016 Enantiodivergent brucine diol-catalyzed 1,3-dipolar cycloaddition of azomethine ylides with α,β-unsaturated ketones. *Adv. Synth. Catal.* **358**, 984–993. (doi:10.1002/adsc.201500958)

6. Luo S, Zhang N, Wang Z, Yan H. 2018 Enantioselective addition of selenosulfonates to α,β-unsaturated ketones. *Org. Biomol. Chem.* **16**, 2893–2901. (doi:10.1039/C8OB00359A)

7. Syamala LVRB, Khopade TM, Warghude PK, Bhat RG. 2019 An access to α, β-unsaturated ketones via dual cooperative catalysis. *Tetrahedron Lett.* **60**, 88–91. (doi:10.1016/j.tetlet.2018.11.064)

8. Kollár L, Pongrácz P. 2018 Tandem hydroformylation/aldol condensation reactions: synthesis of unsaturated ketones from olefins. *J. Organomet. Chem.* **866**, 184–188. (doi:10.1016/j.jorganchem.2018.04.031)

9. Khopade TM, Warghude PK, Mete TB, Bhat RG. 2019 Acyl/aroyl Meldrum's acid as an enol surrogate for the direct organocatalytic synthesis of α,β-unsaturated ketones. *Tetrahedron Lett.* **60**, 197–200. (doi:10.1016/j.tetlet.2018.12.013)

10. Sharley JS, Pérez AMC, Ferri EE, Miranda AF, Baxendale IR. 2016 α,β-Unsaturated ketones via copper(II) bromide mediated oxidation. *Tetrahedron* **72**, 2947–2954. (doi:10.1016/j.tet.2016.04.011)

11. Mameda N, Peraka S, Kodumuri S, Chevella D, Banothu R, Amrutham V, Nam N. 2016 Synthesis of α,β-unsaturated ketones from alkynes and aldehydes over Hβ zeolite under solvent-free conditions. *RSC Adv.* **6**, 58 137–58 141. (doi:10.1039/C6RA11593D)

12. Kuga T, Sasano Y, Iwabuchi Y. 2018 IBX as a catalyst for dehydration of hydroperoxides:

green entry to α,β-unsaturated ketones *via* oxygenative allylic transposition. *Chem. Commun.* **54**, 798–801. (doi:10.1039/C7CC08957K)

13. Song B, Xu B. 2017 Metal-catalyzed C–H functionalization involving isocyanides. *Chem. Soc. Rev.* **46**, 1103–1123. (doi:10.1039/C6CS00384B)

14. Shi R, Niu H, Lu L, Lei A. 2017 Pd/Cu-catalyzed aerobic oxidative aromatic C–H bond activation/N-dealkylative carbonylation towards the synthesis of phenanthridinones. *Chem. Commun.* **53**, 1908–1911. (doi:10.1039/C6CC08701A)

15. Wang F, Yu S, Li X. 2016 Transition metal-catalysed couplings between arenes and strained or reactive rings: combination of C–H activation and ring scission. *Chem. Soc. Rev.* **45**, 6462–6477. (doi:10.1039/C6CS00371K)

16. Wang J, Liu C, Yuan J, Lei A. 2013 Copper-catalyzed oxidative coupling of alkenes with aldehydes: direct access to α,β-unsaturated ketones. *Angew. Chem. Int. Ed.* **52**, 2256–2259. (doi:10.1002/anie.201208920)

17. Arandiyan H, Wang Y, Sun H, Rezaei M, Dai H. 2018 Ordered meso- and macroporous perovskite oxide catalysts for emerging applications. *Chem. Commun.* **54**, 6484–6502. (doi:10.1039/C8CC01239C)

18. Li T, Pan Y, Wang Z, Xia Y, Chen Y, Huang W. 2017 Additive engineering for highly efficient organic–inorganic halide perovskite solar cells: recent advances and perspectives. *J. Mater. Chem. A* **5**, 12 602–12 652. (doi:10.1039/C7TA01798G)

19. Miao J, Zhang F. 2019 Recent progress on highly sensitive perovskite photodetectors. *J. Mater. Chem. C* **7**, 1741–1791. (doi:10.1039/C8TC06089D)

20. Jung M, Ji S-G, Kim G, Seok SI. 2019 Perovskite precursor solution chemistry: from fundamentals to photovoltaic applications. *Chem. Soc. Rev.* **48**, 2011–2038. (doi:10.1039/C8CS00656C)

21. Wei Y, Cheng Z, Lin J. 2019 An overview on enhancing the stability of lead halide perovskite quantum dots and their applications in phosphor-converted LEDs. *Chem. Soc. Rev.* **48**, 310–350. (doi:10.1039/C8CS00740C)

22. Huang X, Zhao G, Wang G, Irvine JTS. 2018 Synthesis and applications of nanoporous perovskite metal oxides. *Chem. Sci.* **9**, 3623–3637. (doi:10.1039/C7SC03920D)

23. Shin H, Baek M, Kim DH. 2019 Sulfur resistance of Ca-substituted $LaCoO_3$ catalysts in CO oxidation. *Mol. Catalysis* **468**, 148–153. (doi:10.1016/j.mcat.2019.02.020)

24. Chagas CA, Toniolo FS, Magalhães RNSH, Schmal M. 2012 Alumina-supported $LaCoO_3$ perovskite for selective CO oxidation (SELOX). *Int. J. Hydrogen Energ.* **37**, 5022–5031. (doi:10.1016/j.ijhydene.2011.12.052)

25. Seyfi B, Baghalha M, Kazemian H. 2009 Modified $LaCoO_3$ nano-perovskite catalysts for the environmental application of automotive CO oxidation. *Chem. Eng. J.* **148**, 306–311. (doi:10.1016/j.cej.2008.08.041)

26. Wang X *et al.* 2018 Activation of surface oxygen sites in a cobalt-based perovskite model catalyst for CO oxidation. *J. Phys. Chem. Lett.* **9**, 4146–4154. (doi:10.1021/acs.jpclett.8b01623)

27. Yadav PK, Das T. 2019 Production of syngas from carbon dioxide reforming of methane by using $LaNi_xFe_{1-x}O_3$ perovskite type catalysts. *Int. J. Hydrogen Energ.* **44**, 1659–1670. (doi:10.1016/j.ijhydene.2018.11.108)

28. Wang H, Dong X, Zhao T, Yu H, Li M. 2019 Dry reforming of methane over bimetallic Ni-Co catalyst prepared from $La(Co_xNi_{1-x})_{0.5}Fe_{0.5}O_3$ perovskite precursor: catalytic activity and coking resistance. *Appl. Catal. B Environ.* **245**, 302–313. (doi:10.1016/j.apcatb.2018.12.072)

29. Kim WY, Jang JS, Ra EC, Kim KY, Kim EH, Lee JS. 2019 Reduced perovskite $LaNiO_3$ catalysts modified with Co and Mn for low coke formation in dry reforming of methane. *Appl. Catal. A Gen.* **575**, 198–203. (doi:10.1016/j.apcata.2019.02.029)

30. Valderrama G, Kiennemann A, Navarro CUd, Goldwasser MR. 2018 $LaNi_{1-x}Mn_xO_3$ perovskite-type oxides as catalysts precursors for dry reforming of methane. *Appl. Catal. A Gen.* **565**, 26–33. (doi:10.1016/j.apcata.2018.07.039)

31. Guldal NO, Figen HE, Baykara SZ. 2017 Production of hydrogen from hydrogen sulfide with perovskite type catalysts: $LaMO_3$. *Chem. Eng. J.* **313**, 1354–1363. (doi:10.1016/j.cej.2016.11.057)

32. Guldal NO, Figen HE, Baykara SZ. 2018 Perovskite catalysts for hydrogen production from hydrogen sulfide. *Int. J. Hydrogen Energ.* **43**, 1038–1046. (doi:10.1016/j.ijhydene.2017.10.156)

33. Kwon BW, Oh JH, Kim GS, Yoon SP, Han J, Nam SW, Ham HC. 2018 The novel perovskite-type Ni-doped $Sr_{0.92}Y_{0.08}TiO_3$ catalyst as a reforming biogas ($CH_4 + CO_2$) for H_2 production. *Appl. Energ.* **227**, 213–219. (doi:10.1016/j.apenergy.2017.07.105)

34. Pan KL, Pan GT, Chong S, Chang MB. 2018 Removal of VOCs from gas streams with double perovskite-type catalysts. *J. Environ. Sci.* **69**, 205–216. (doi:10.1016/j.jes.2017.10.012)

35. Meng Q, Wang W, Weng X, Liu Y, Wang H, Wu Z. 2016 Active oxygen species in $La_{n+1}Ni_nO_{3n+1}$ layered perovskites for catalytic oxidation of toluene and methane. *J. Phys. Chem. C* **120**, 3259–3266. (doi:10.1021/acs.jpcc.5b08703)

36. Liu L, Zhang H, Jia J, Sun T, Sun M. 2018 Direct molten polymerization synthesis of highly active samarium manganese perovskites with different morphologies for VOC removal. *Inorg. Chem.* **57**, 8451–8457. (doi:10.1021/acs.inorgchem.8b01125)

37. Garcia-Muñoz P, Lefevre C, Robert D, Keller N. 2019 Ti-substituted $LaFeO_3$ perovskite as photoassisted CWPO catalyst for water treatment. *Appl. Catal. B Environ.* **248**, 120–128. (doi:10.1016/j.apcatb.2019.02.030)

38. Wang W, Tadé MO, Shao Z. 2015 Research progress of perovskite materials in photocatalysis- and photovoltaics-related energy conversion and environmental treatment. *Chem. Soc. Rev.* **44**, 5371–5408. (doi:10.1039/C5CS00113G)

39. Wang WL, Meng Q, Xue Y, Weng X, Sun P, Wu Z. 2018 Lanthanide perovskite catalysts for oxidation of chloroaromatics: secondary

pollution and modifications. *J. Catal.* **366**, 213–222. (doi:10.1016/j.jcat.2018.07.022)

40. Dükkancı M. 2018 Sono-photo-Fenton oxidation of bisphenol-A over a $LaFeO_3$ perovskite catalyst. *Ultrason. Sonochem.* **40**, 110–116. (doi:10.1016/j.ultsonch.2017.04.040)

41. Wu X, Yu J, Yang G, Liu H, Zhou W, Shao Z. 2018 Perovskite oxide/carbon nanotube hybrid bifunctional electrocatalysts for overall water splitting. *Electrochim. Acta* **286**, 47–54. (doi:10.1016/j.electacta.2018.08.010)

42. Adnan MAB, Arifin K, Minggu LJ, Kassim MB. 2018 Titanate-based perovskites for photochemical and photoelectrochemical water splitting applications: a review. *Int. J. Hydrogen Energ.* **43**, 23 209–23 220. (doi:10.1016/j.ijhydene.2018.10.173)

43. Can E, Yildirim R. 2018 Data mining in photocatalytic water splitting over perovskites literature for higher hydrogen production. *Appl. Catal. B Environ.* **242**, 267–283. (doi:10.1016/j.apcatb.2018.09.104)

44. Wu D, Zhang X, Jing Y, Zhao X, Zhou Z. 2016 Towards visible-light water splitting photocatalysts: band engineering of two-dimensional $A_5B_4O_{15}$ perovskites. *Nano Energ.* **28**, 390–396. (doi:10.1016/j.nanoen.2016.08.064)

45. Lu F, Xia T, Li Q, Wang J, Huo L, Zhao H. 2019 Heterostructured simple perovskite nanorod-decorated double perovskite cathode for solid oxide fuel cells: highly catalytic activity, stability and CO_2-durability for oxygen reduction reaction. *Appl. Catal. B Environ.* **249**, 19–31. (doi:10.1016/j.apcatb.2019.02.056)

46. Yuan R-h, He Y, He W, Ni M, Leung MKH. 2019 $La_{0.8}Sr_{0.2}MnO_3$ based perovskite with A-site deficiencies as high performance bifunctional electrocatalyst for oxygen reduction and evolution reaction in alkaline. *Energy Procedia* **158**, 5804–5810. (doi:10.1016/j.egypro.2019.01.548)

47. Safakas A, Bampos G, Bebelis S. 2019 Oxygen reduction reaction on $La_{0.8}Sr_{0.2}Co_xFe_{1-x}O_{3-\delta}$ perovskite/carbon black electrocatalysts in alkaline medium. *Appl. Catal. B Environ.* **244**, 225–232. (doi:10.1016/j.apcatb.2018.11.015)

48. Kim WS, Anoop G, Lee HJ, Lee SS, KwakHye JH, Lee J, Jo JY. 2016 Facile synthesis of perovskite $LaMnO_{3+\delta}$ nanoparticles for the oxygen reduction reaction. *J. Catal.* **344**, 578–582. (doi:10.1016/j.jcat.2016.10.029)

49. Onrubia JA, Pereda-Ayo B, De-La-Torre U, González-Velasco JR. 2017 Key factors in Sr-doped $LaBO_3$ (B=Co or Mn) perovskites for NO oxidation in efficient diesel exhaust purification. *Appl. Catal. B Environ.* **213**, 198–210. (doi:10.1016/j.apcatb.2017.04.068)

50. Jung WY, Hong S-S. 2013 Synthesis of $LaCoO_3$ nanoparticles by microwave process and their photocatalytic activity under visible light irradiation. *J. Ind. Eng. Chem.* **19**, 157–160. (doi:10.1016/j.jiec.2012.07.018)

51. Ao M, Pham GH, Sage VE, Pareek V. 2016 Structure and activity of strontium substituted $LaCoO_3$ perovskite catalysts for syngas conversion. *J. Mol. Catal. A Chem.* **416**, 96–104. (doi:10.1016/j.molcata.2016.02.020)

52. Escalona N, Fuentealba S, Pecchi G. 2010 Fischer–Tropsch synthesis over $LaFe_{1-x}Co_xO_3$

perovskites from a simulated biosyngas feed. *Appl. Catal. A Gen.* **381**, 253–260. (doi:10.1016/j.apcata.2010.04.022)

53. Sun M, Jiang Y, Li F, Xia M, Xue B, Liu D. 2010 Dye degradation activity and stability of perovskite-type $LaCoO_{3-x}$ (x=0∼0.075). *Mater. Transactions* **51**, 2208–2214. (doi:10.2320/matertrans.M2010200)

54. Sarker AR. 2015 Synthesis of high quality $LaCoO_3$ crystals using water based sol-gel method. *Int. J. Mater. Sci. Appl.* **4**, 159–164. (doi:10.11648/j.ijmsa.20150403.13)

55. Zhou C, Feng Z, Zhang Y, Hu L, Chen R, Shan B, Yin H, Wang WG, Huang A. 2015 Enhanced

catalytic activity for NO oxidation over Ba doped $LaCoO_3$ catalyst. *RSC Adv.* **5**, 28 054–28 059. (doi:10.1039/C5RA02344K)

56. Dyson PJ, Jessop PG. 2016 Solvent effects in catalysis: rational improvements of catalysts via manipulation of solvent interactions. *Catal. Sci. Technol.* **6**, 3302–3316. (doi:10.1039/C5CY02197A)

57. Zhu Y, Wei Y. 2014 Copper catalyzed direct alkenylation of simple alkanes with styrenes. *Chem. Sci.* **5**, 2379–2382. (doi:10.1039/c4sc00093e)

58. Teng F, Sun S, Jiang Y, Yu J-T, Cheng J. 2015 Copper-catalyzed oxidative C(sp₃)–H/N–H

coupling of sulfoximines and amides with simple alkanes via a radical process. *Chem. Commun.* **51**, 5902–5905. (doi:10.1039/C5CC00839E)

59. Liu Q, Jackstell R, Beller M. 2013 Oxidative catalytic coupling reactions: selective formation of C–C and C–X bonds using radical processes. *Angew. Chem. Int. Ed.* **52**, 13 871–13 873. (doi:10.1002/anie.201307865)

60. Zhang HM. 1990 Oxygen sorption and catalytic properties of $La_{1-x}Sr_xCo_{1-y}Fe_yO_3$ perovskite-type oxides. *J. Catal.* **121**, 432–440. (doi:10.1016/0021-9517(90)90251-E)